INSTABILITY AND ENERGETICS IN A BAROCLINIC OCEAN

by

Kuh Kim

S.B., Seoul National University
(1968)

M.S., Seoul National University
(1970)

SUBMITTED IN PARTIAL FULFILLMENT OF THE
REQUIREMENTS FOR THE DEGREE OF
DOCTOR OF PHILOSOPHY

at the

MASSACHUSETTS INSTITUTE OF TECHNOLOGY

and the

WOODS HOLE OCEANOGRAPHIC INSTITUTION

August, 1975

Signature of Author.....
Joint Program in Oceanography, Massachusetts Institute of Technology - Woods Hole Oceanographic Institution, and Department of Earth and Planetary Sciences, and Department of Meteorology, Massachusetts Institute of Technology, August 1975

Certified by... ....
Thesis Supervisor

Accepted by..... ....
Chairman, Joint Oceanography Committee in the Earth Sciences, Massachusetts Institute of Technology - Woods Hole Oceanographic Institution

INSTABILITY AND ENERGETICS IN A BAROCLINIC OCEAN

by

Kuh Kim

Submitted to the Massachusetts Institute of Technology-Woods Hole Oceanographic Institution Joint Program in Oceanography on August 11, 1975, in partial fulfillment of the requirements for the degree of Doctor of Philosophy.

ABSTRACT

This thesis is made of two separate, but interrelated parts.

In Part I the instability of a baroclinic Rossby wave in a two-layer ocean of inviscid fluid without topography, is investigated and its results are applied in the ocean. The velocity field of the basic state (the wave) is characterized by significant horizontal and vertical shears, non-zonal currents, and unsteadiness due to its westward propagation. This configuration is more relevant to the ocean than are the steady, zonal 'meteorological' flows, which dominate the literature of baroclinic instability. Truncated Fourier series are used in perturbation analyses.

The wave is found to be unstable for a wide range of the wavelength; growing perturbations draw their energy from kinetic or potential energy of the wave depending upon whether the wavelength, $2\pi L$, is much smaller or larger than $2\pi L_\rho$, respectively, where L_ρ is the internal radius of deformation. When the shears are comparable dynamically, $L \sim L_\rho$, the balance between the two energy transfer processes is very sensitive to the ratios L/L_ρ and U/C as well, where U is a typical current speed, and C a typical phase speed of the wave. For $L = L_\rho$ they are augmenting if $U < C$, yet they detract from each other if $U > C$.

The beta-effect tends to stabilize the flow, but perturbations dominated by a zonal velocity can grow irrespective of the beta-effect.

It is necessary that growing perturbations are comprised of both barotropic and baroclinic modes vertically. The scale of the fastest growing perturbation is significantly larger than L for barotropically controlled flows ($L < L_\rho$), reduces to the wave scale L for a mixed kind ($L \sim L_\rho$) and is fixed slightly larger than L_ρ for baroclinically controlled flows ($L > L_\rho$).

Increasing supply of potential energy causes the normalized growth rate, $\alpha L/U$, to increase monotonically as $L \to L_\rho$ from below. As L increases further beyond L_ρ, the growth rate $\alpha L_\rho/U$ shows a slight increase, but soon approaches an asymptotic value.

In a geophysical eddy field like the ocean this model shows possible pumping of energy into the radius of deformation ($\sim$ 40 km rational scale, or 250 km wavelength) from both smaller and larger scales through nonlinear interactions, which occur without interference from the beta-effect. The e-folding time scale is about 24 days if U = 5 cm/sec and L = 90 km. Also it is strongly suggested that, given the observed distribution of energy versus length scale, eddy-eddy interactions are more vigorous than eddy-mean interaction, away from intense currents like the Gulf Stream. The flux of energy toward the deformation scale, and the interaction of barotropic and baroclinic modes, occur also in fully turbulent 'computer' oceans, and these calculations provide a theoretical basis for source of these experimental cascades.

In Part II an available potential energy (APE) is defined in terms appropriate to a limited area synoptic density map (e.g., the 'MODE-I' data) and then in terms appropriate to time-series of hydrographic station at a single geographic location (e.g., the 'Panulirus' data).

Instantaneously the APE shows highly variable spatial structure, horizontally as well as vertically, but the vertical profile of the average APE from 19 stations resembles the profile of vertical gradient of the reference stratification. The eddy APE takes values very similar to those of the average kinetic energy density at 500 m, 1500 m and 3000 m depth in the MODE area.

In and above the thermocline the APE has roughly the same level in the MODE area (centered at 28°N, 69° 40'W) as at the Panulirus station (32° 10'N, 64° 30'W), yet in the deep water there is significantly more APE at the Panulirus station. This may in part indicate an island effect near Bermuda.

Thesis Supervisor: Peter B. Rhines
Title: Senior Scientist, Department of Physical Oceanography,
Woods Hole Oceanographic Institution.

ACKNOWLEDGMENTS

The author wishes to express sincere thanks to Dr. Peter Rhines for providing a unique opportunity to work under his supervision. From the initial motivation to the completion of this thesis, Dr. Rhines has been a constant source of encouragement and physical insight. Thanks are also expressed to Professor Jule Charney and Professor John Hart at M.I.T. for the constructive comments which were very important in expanding the scope of the research. Professor Carl Wunsch also at M.I.T. kindly provided the edited Panulirus data. Ms. Elizabeth Schroeder at the Woods Hole Oceanographic Institution made available the current unpublished results of the Panulirus data, which have been a great help. A special word of thanks must be extended to Ms. Audrey Williams and Ms. Doris Haight for their superb help in typing this thesis.

This research has been supported by the National Science Foundation grant IDO 73-09737, formerly GX-36342. The support is gratefully acknowledged.

TABLE OF CONTENTS

		Page
ABSTRACT		2
ACKNOWLEDGMENTS		4
LIST OF FIGURES		7
LIST OF TABLES		13
PART I		14
I.	INTRODUCTION	15
II.	BASIC FORMULATION	35
II-1	Basic Equations in a Two-layer Ocean	35
II-2	Energy Conservation	43
II-3	Exact Solutions of the Basic Equations and Their Stability	45
III.	PERTURBATION EQUATIONS	49
III-1	Linearized Perturbation Equations	49
III-2	Energy Equation for the Perturbation	52
III-3	Integral Properties of Perturbation	54
IV.	PERTURBATION ANALYSIS	60
IV-1	Solutions in Fourier Series	60
IV-2	Characteristics in 3-mode Truncation	68
IV-2-1	Marginal Stability Curves	68
IV-2-2	Growth Rate for Unstable Perturbation	71
IV-3	Higher-mode Analysis	80
IV-3-1	Analysis with 7 Modes	81
IV-3-2	Baroclinic Interaction vs. Barotropic Interaction	92
V.	DISCUSSIONS AND GEOPHYSICAL APPLICATIONS	96
VI.	CONCLUSIONS	114
PART II		117
I.	INTRODUCTION	118
II.	DEFINITION OF AVAILABLE POTENTIAL ENERGY	124

		Page
III.	APPLICATION OF THE AVAILABLE POTENTIAL ENERGY . .	134
III-1	Available Potential energy in the MODE Area	134
III-1-1	Mean Density Field	136
III-1-2	Eddy Available Potential Energy	139
III-2	Available Potential Energy from the Panulirus Data	149
III-2-1	Anomaly of Potential Energy	150
III-2-2	Eddy Available Potential Energy	156
IV.	DISCUSSION AND CONCLUSIONS	164
BIBLIOGRAPHY	. . . . .	169
BIOGRAPHY	. . . . .	175

LIST OF FIGURES

Figure		Page
Part I		
1.1	From Crease(1962). Trajectories of five series of floats. Figures at ends of trajectory are starting and finishing dates. Figures beside trajectory are average speeds. Currents are very energetic with an apparent period of 50 to 100 days(Swallow,1971) and an estimated wavelength of 300 to 400 km(Phillips,1966).	18
1.2	From Schroeder and Stommel(1969). Temperature anomalies at the Panulirus station in 1960. Units: hundreds of a degree centigrade. Vertical scale changes at 200 m. Closed contours in the thermocline show a strong temporal variation. Anomaly of 1°C roughly corresponds to a vertical excursion of 50 m in the thermocline.	19
1.3	From Wunsch(1972a). Spectrum of temperature near Bermuda near the depth of the main thermocline, plotted so that the area under the curve is proportional to the variance of temperature. Most of the energy lies in periods of 40-200 days, indicating a strong low frequency variation.	20
1.4	Depth of 10°C isotherm from the data in Fuglister(1960). Sampling is sparse, but the presence of multiple scales is apparent at two separate sections.	21
1.5	From Katz(1973). Depth of isopycnals, σ_t= 26.91 for Tow 300 and σ_t=26.87 for Tow 400. These profiles confirm the presence of an intermediate scale. The distance between a peak and a valley is 180 km from Tow 400 and 360 km from Tow 300 at least.	23
1.6	Profile of mean speed and mean velocity plotted from Koshlyakov and Grachov(1973). A large-scale anti-cyclonic eddy was observed during the Polygon experiment and its mean speed is overwhelmingly larger than mean velocity for all depth. The main thermocline is located at about 250 m.	24

Figure		Page
1.7	From Sanford(1975). Velocity profiles show a strong shear concentrated in the main thermocline, suggesting the dominance of grave baroclinic mode.	26
1.8	From Veronis and Stommel(1956). The dispersion relations of barotropic and baroclinic Rossby waves in a two-layer ocean. Thicknesses of upper and lower layers are 500 m and 3500 m, respectively. $f=10^{-4}$ sec^{-1}, $\beta=2\times10^{-13}$ cm^{-13}sec^{-1}. The radius of deformation based upon the upper layer thickness is 31 km. Note that the minimum period of the baroclinic Rossby wave is about one year.	29
2.1	The stratification of the ocean is idealized by two homogeneous layers of densities, ρ_1 and ρ_2, where $\rho_1 < \rho_2$. Thickness of the upper layer is h_1 and h_2 is a height of the interface.	36
3.1	The velocity structure of the basic wave is characterized by the presence of horizontal shear as well as vertical shear, associated with kinetic and potential energies respectively, which are partitioned by $(L_\rho/L)^2$, where L_ρ is the internal radius of deformation.	50
4.1	Branch I: The regime above marginal stability curves is unstable and one below the curves is stable. Note short wavelength limit of unstable perturbations in the meridional scale of perturbation(L_p) for large scale basic flow, $L > L_\rho$. There exist unstable modes irrespective of the current strength U. Branch II: The unstable region is both upper and lower bounded in L_p/L_ρ. As in Branch I, unstable perturbation exists for $\frac{U}{C} < 1$.	69
4.2a	The beta-effect(β) is relatively strong and the baroclinic and barotropic instability regimes are distinct for very large and small value of L/L_ρ, respectively. The restoring effect of β clearly acts to stabilize modes near the center of the figure.	72

Figure		Page
4.2b	As the basic flow strengthens (or with a weak beta-effect), the baroclinic and barotropic instability regimes merge into a smooth growth-surface. Short wavelength limit in the baroclinic regime is shown clearly,	73
4.2c	Same as Fig. 4.2b except for a stronger current case. The meridional scale of the fastest growing perturbation is fixed at a scale slightly larger than the radius of deformation in the baroclinic regime and decreases in proportional to the zonal scale of the basic flow in the barotropic regime.	74
4.3	Growth rate $\alpha L/U$, renormalized for the range $L \leq L_\rho$, where the barotropic interaction is important. The scale at the maximum growth rate is the same as that of the basic flow for $\frac{U}{C} = \infty$ and $\frac{L}{L_\rho} = 1$ and the basic flow generates a larger scale as its scale and strength decrease.	76
4.4	Recapitulation of Fig. 4.3. Figures beside the curves are values of U/C and L_p/L at the maximum growth rate. Note an increase of the growth rate as $L \to L_\rho$, which is possible because of of an increasing supply of potential energy.	77
4.5	These curves correspond to vertical cuts in Fig. 4.2b(3-mode). Growth rate shows basically the same behavior as found from the 3-mode analysis; short wavelength limit and maximum growth rate at $L_p \simeq L_\rho$ in baroclinically controlled flows, and generation of larger scale in a barotropically controlled flow.	82
4.6	For region $L < L_\rho$ this figure is very similar to Fig. 4.4 from the 3-mode analysis, indicating truncation errors are small. For $L > L_\rho$, a slight decrease of normalized growth rate as $L \to L_\rho$ from above is notable. This may be due to a feedback of energy into the basic wave via the interaction of Reynold stresses with the mean horizontal shear.	84

Figure — Page

4.7 From Simmons(1974). The dependence of maximum growth rate on channel width for a steady, zonal current with profile $u = 1 - 4\delta(\frac{y}{y_o} - \frac{1}{2})^2$, where meridional walls are at $y = 0, y_o$. Lower layer is at rest initially and the radius of deformation is 1,225 km. Note a reduction of growth rate due to a non-uniformity ($\delta \neq 0$) compared with the case $\delta = 0$. As the channel becomes narrower (a horizontal shear increases effectively), the growth rate decreases further, meanwhile the horizontal shear is intensified. 86

4.8a Fast convergence of series for $U < C$ and $L < L_\rho$ answers why the results from the 3-mode analysis are so close to those from the 7-mode one. Convergence becomes slower as L increases from L_ρ and U from C. However, a calculation with 9 modes show very little further change in the growth rate. 88

4.8b A tendency to generate a strong barotropic component of growing perturbation can be more easily seen in Branch II. Odd modes, $n = \pm 1, \pm 3, \cdots\cdots$, are barotropic vertically. 89

4.9 Relative perturbation kinetic energy plotted as a scalar wavenumber spectrum. Wavenumber unity corresponds to the deformation radius and the wavenumber of the basic wave is underlined. Irrespective of U/C and L/L_ρ, mode n = 0, the lowest wavenumber representing the zonal component of the perturbation, contributes the highest peak. It is interesting to produce a quasi-continuous spectrum from a single mode. 91

4.10 The balance between the two distinct energy transfer processes is very sensitive to the ratios L/L_ρ and U/C as well. Potential energy of the wave is always available for growing perturbations, yet kinetic energy of the wave is not. Note a feedback of energy toward the wave for a strong current, $\frac{U}{C} = 2.5$. 94

Figure		Page
5.1	Rhines' (1975a) numerical experiment shows that a large-scale baroclinic Rossby wave with $L \cong 4 \times L_\rho$ is unstable and 'noise' develops into eddy field. Slow westward propagation of stream lines are visible along left and right edges. At t = 1.0 (about 23 days later) organized eddy field can be identifiable and further amplification is very clear at t = 1.5.	105
5.2	Perturbation energy grows exponentially as predicted in the theory during the instability shown in Fig. 5.1.	106
5.3	Energy transfer during the instability shown in Fig. 5.1 is dominated by the baroclinic process. Barotropic interaction removes kinetic energy from wavenumber 6, but the net kinetic energy increases via the conversion from the potential energy at the same wavenumber supplied from wavenumber 2 by the instability.	108
5.4	Initially energy spectrum has two peaks, one at k = 1 and the other around k = 6. Subsequent energy transfers toward higher wavenumbers (k = 8 corresponds to the radius of deformation) are concentrated around k = 6 with very little change at k = 1. This development is consistent with the theoretical prediction.	109
Part II		
2.1	An available potential energy (APE) is defined as work done by a local mean buoyancy force $\frac{1}{2}g\rho'$ for a displacement of $z - z_p$, where ρ' is approximated by $-\bar{\rho}_z(z-z_p)$. Note that the APE is positive definite. Accordingly each fluid particle has its own reference level in the definition of the APE.	129
3.1a	Comparison of 5 Chain station data with 5 Researcher station data on the circle of 200 km in radius in March, 1973. Statistical test shows that the difference in the average potential density is not significant for a 95% confidence interval.	140

Figure		Page
3.1b	Same as Fig. 3.1a, except that salinity and temperature are intercompared. The results of statistical tests are the same as that for the potential density.	141
3.2	The APE varies very significantly in space, horizontally as well as vertically.	142
3.3	Profile of an average APE in space from 19 stations shows remarkably simple vertical structure, which resembles the profile of vertical gradient of the reference stratification. This energy level is very similar to the average kinetic energy density at 500 m, 1500 m and 3000 m depth.	144
3.4	Estimates of r.m.s. vertical excursion reveal large vertical movements below the thermocline, suggesting a strong baroclinicity, which seems to contradict the simplified picture sometimes given, that the deep water is dominated by the barotropic mode.	145
3.5a	Variation of the APE over a scale of 100 km suggests that an advection of the APE could be very important in a local energetics.	146
3.5b	Same as Fig. 3.5a, but in June.	147
3.6	Monthly variation of the mean anomaly of potential energy.	152
3.7	Time-series of fluctuating part(χ') of the anomaly of potential energy. The fluctuations are strongly coupled between the two layers. Over all the lower layer has a smaller amplitude of variation than the upper layer, yet they are of the same order of 10^8 ergs/cm^2.	153
3.8	Monthly variation of the mean potential density minus the average over 7 years.	155
3.9	Time-series of the APE shows again the coupling between the water in and below the thermocline. Note that a typical magnitude of the APE is smaller than that of the fluctuation in Fig. 3.7 by an order of magnitude at least.	158

Figure Page

3.10 Out of 151 stations the APE is less than the mean for 71% of them and higher for 29%. Irregular burst of high energy contributes the 29%. 162

LIST OF TABLES

Table Page

Part II

1 Anomaly of potential energy at Site D. 121

2a List of CTD and STD stations in March. 137

2b List of CTD and STD stations in June. 138

3 Comparison of the available potential energy with the kinetic energy in the MODE area. 148

PART I

I. INTRODUCTION

Prior to this decade currents in the ocean interior were modelled as a sum of linear Sverdrup flow (Sverdrup, 1947) and linear waves (Veronis and Stommel, 1956). In regions of intense boundary currents nonlinearity was added later (Charney, 1955), and the instability of these currents was examined numerically (Bryan, 1963). However, discoveries of intense space- and time-dependent mid-ocean 'eddies', begun with the Aries measurements in 1959-60, led to growing uncertainty about the linear dynamics of either the mean circulation or the fluctuations.

Some recent theories emphasize a new physics, in which the eddies rapidly alter their horizontal and vertical structures (in the inertial time-scale of a few weeks to a few months). At the same time vestiges of linear wave theory, persistent westward propagation found in numerical experiments and observations, still apply so that there is a dual nature to such eddies.

To capture some of this dual nature we examine the stability of one of the fundamental linear waves, the baroclinic Rossby wave. Intense instability is found in which 'noise' added to the simple wave grows. The resulting transfer of energy to new scales forms a tractable analog of energy cascades in the turbulent numerical models. (The theory was motivated by an experimental demonstration

of the instability by Rhines (1975a)).

In one extreme (large length scale of the basic wave) the instability feeds upon the potential energy of the wave. Classical calculations of baroclinic instability emphasize steady, zonal flows as basic states, which is appropriate to the atmosphere, whereas here we show the effect of an 'oceanic' basic state that is neither steady nor zonal nor infinite in scale.

In another extreme (small initial length scale) the instability feeds on the kinetic energy of the horizontal shear. This limit gives, as a special case, the purely barotropic instability found by Lorenz (1972) and Gill (1974).

At the important intermediate scale (the internal deformation scale $\sim$ 50 km), the instability is of a mixed kind, the two energy sources sometimes augmenting, sometimes detracting from one another.

The application to the ocean suggests (as do the computer experiments) that a given 'eddy' may receive energy from a variety of scales of other eddies as well as from some time-mean flow, and that these 'eddy-eddy' interactions are probably more vigorous than the eddy-mean flow interaction, except in regions of intense currents. The growth-rates of the instability theory are reasonably close to the spectral transfer rates found in turbulence, and the structural similarity of theory and experiments is revealing.

Background

The unexpected discovery of energetic, highly variable currents from the research vessel Aries in the deep western North Atlantic Ocean (Crease, 1962) opened a new chapter in the dynamics of ocean circulation (see Fig. 1.1): the float trajectories revealed relatively high speeds at nominal depths of 2 and 4 km, of the order of 5 to 10 cm/sec, with an apparent period of 50 to 100 days (Swallow, 1971) and an estimated wavelength of 300 to 400 km (Phillips, 1966).

The hydrographic data from the Panulirus station near Bermuda show a very distinct month to month variation of temperature in the main thermocline as shown in Fig. 1.2 (Schroeder and Stommel 1969). The temperature spectrum constructed by Wunsch (1972a) from these data reveals that most of the variance in the main thermocline is located between the periods of 40 to 200 days as shown in Fig. 1.3. This band of periods is certainly in the same range as estimated from the Aries measurements.

In the sections of temperature and salinity from Fuglister (1960) various length scales can be picked by eye. Upon the basin-wide variation is superimposed wiggly structures with scales of hundreds of kilometers. The zonal variations of the 10°C isotherm depth at 24°S and 24°N are shown in Fig. 1.4. Counting the rise and fall of

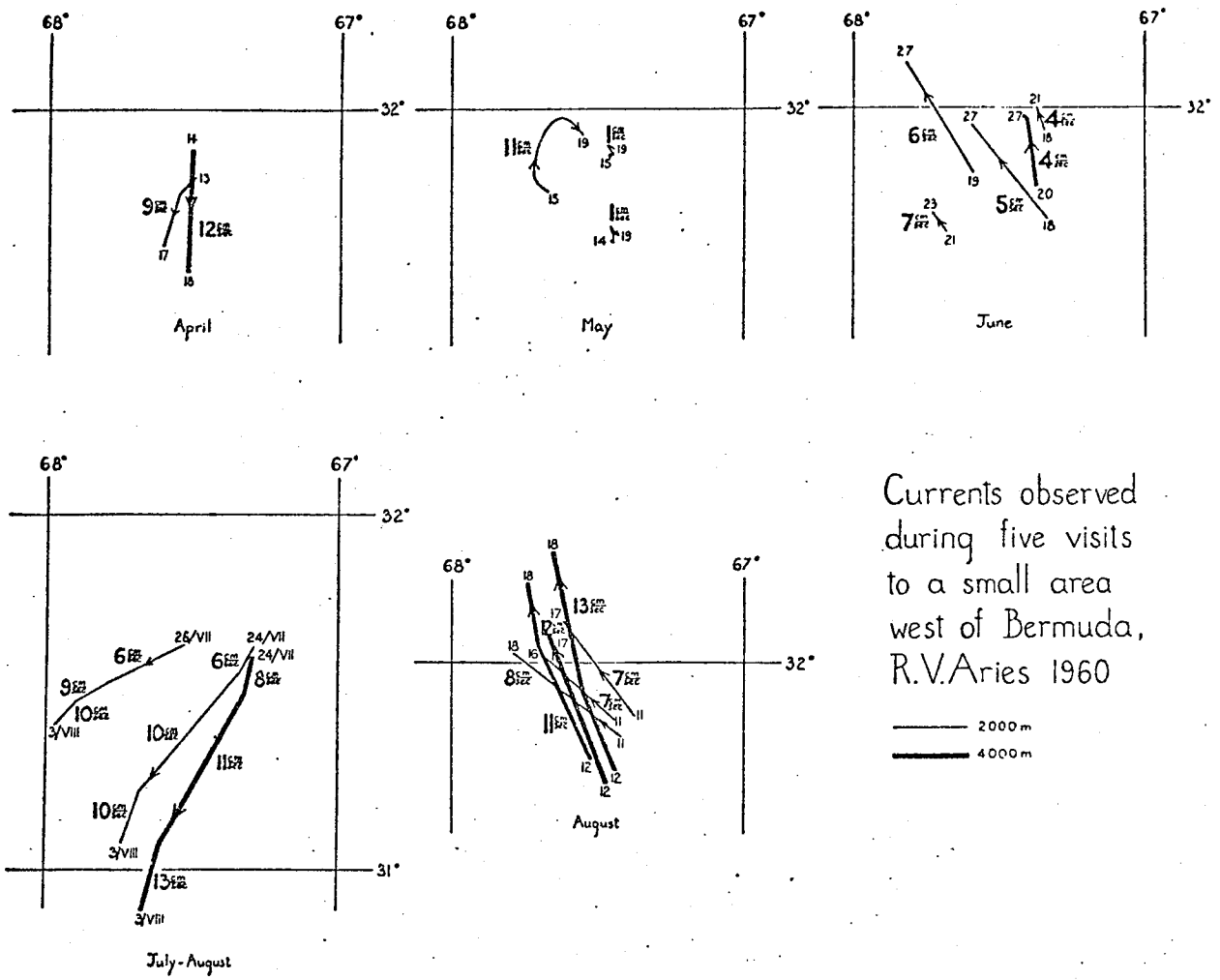

Fig. 1.1 From Crease(1962). Trajectories of five series of floats. Figures at ends of trajectory are starting and finishing dates. Figures beside trajectory are average speeds. Currents are very energetic with an apparent period of 50 to 100 days(Swallow,1971) and an estimated wavelength of 300 to 400 km(Phillips,1966). Current unit is cm/sec.

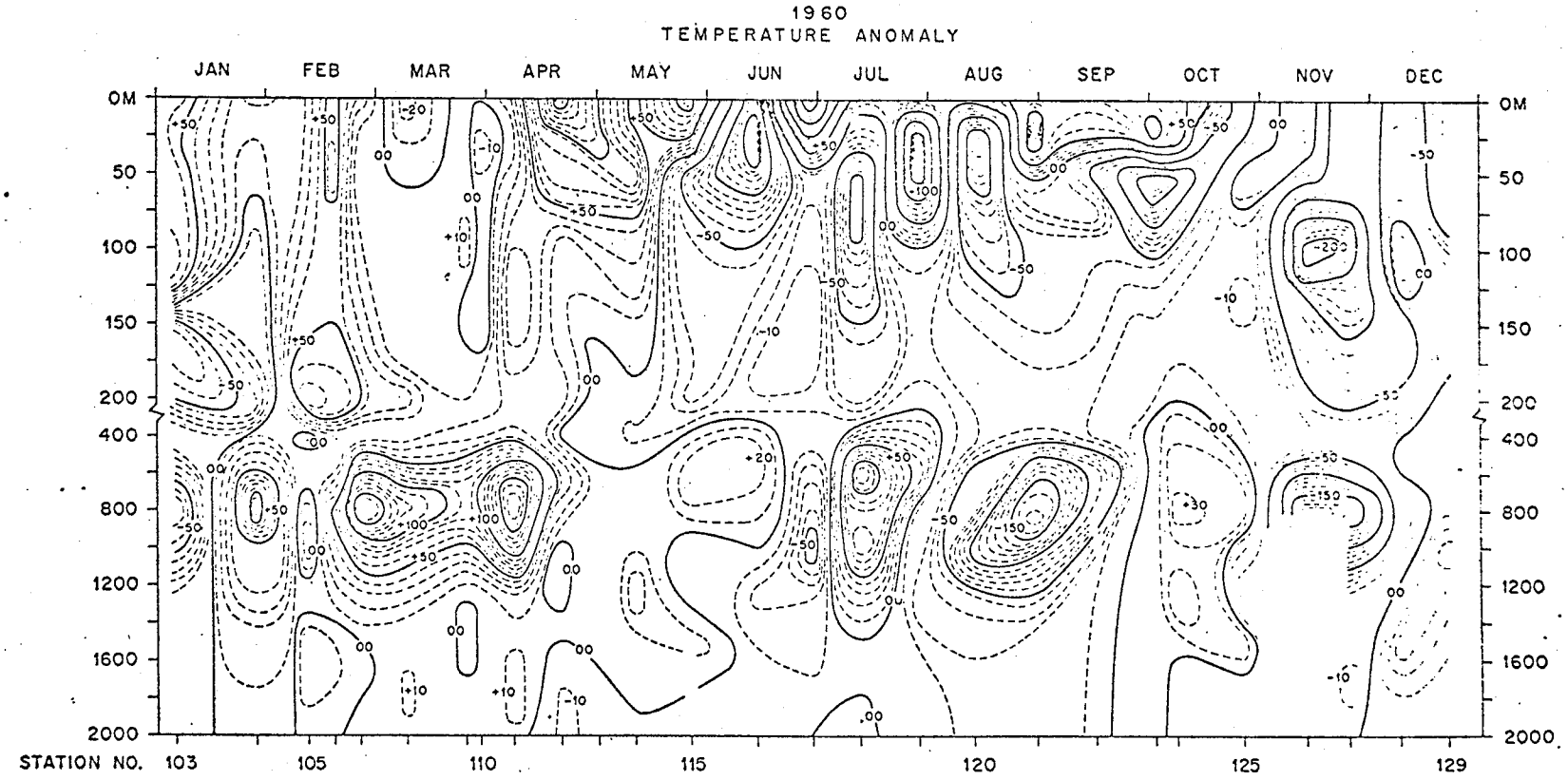

Fig. 1.2 From Schroeder and Stommel(1969). Temperature anomalies at the Panulirus station in 1960. Units: hundreds of a degree centigrade. Vertical scale changes at 200 m. Closed contours in the thermocline shoe a strong temporal variation. Anomaly of 1°C roughly corresponds to a vertical excursion of 50 m in the thermocline.

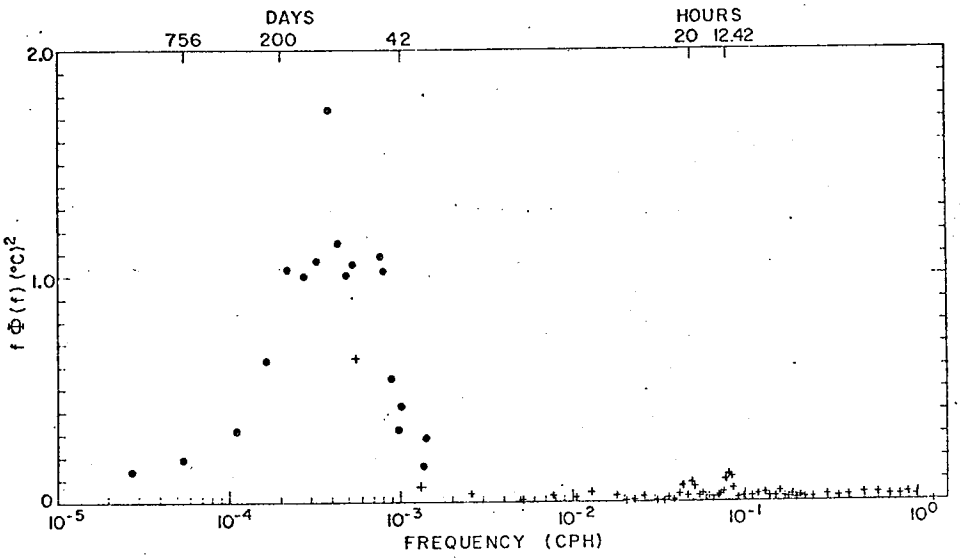

Fig. 1.3 From Wunsch(1972). Spectrum of temperature near Bermuda near the depth of the main thermocline, plotted so that the area under the curve is proportional to the variance of temperature. Most of the energy lies in periods of 40-200 days, indication a strong low frequency variation.

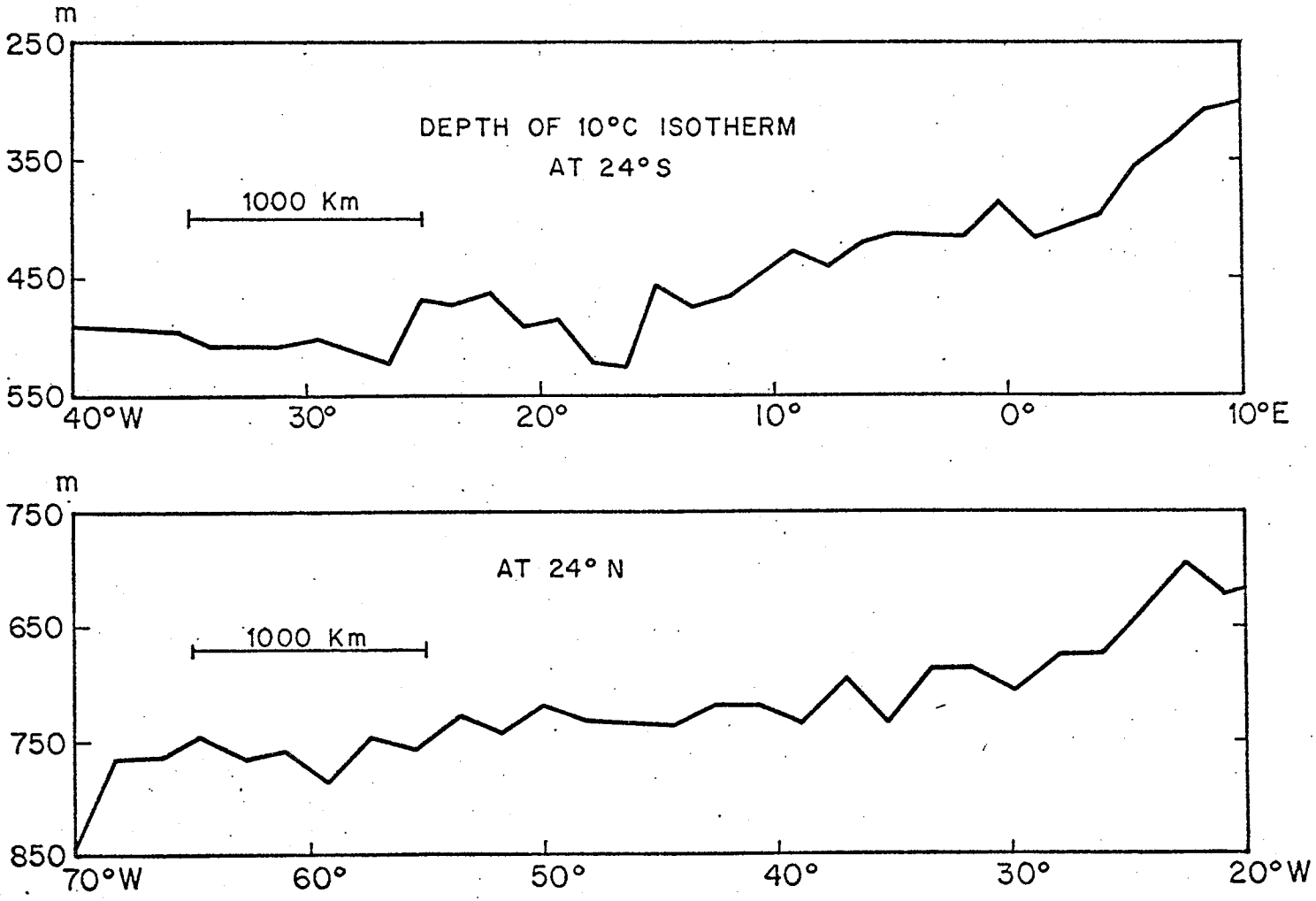

Fig. 1.4 Depth of 10°C isotherm from the data in Fuglister(1960). Sampling is sparse, but the presence of multiple scales is apparemt at two separate sections.

the isotherm depth greater than 20 m between consecutive samplings, there are four minima at 24°S and six at 24°N over 5077 km. The distance between the minima varies from about 600 to 1000 km at 24°S and from about 450 to 1100 km at 24°N. Because of sparse sampling the horizontal resolution is inadequate to show the kind of variation corresponding to the Aries measurements. Nevertheless these comparisons are suggestive in implying the presence of multiple scales at two separated sections.

Katz's (1973) experiments have confirmed the presence of an intermediate scale in the open ocean in Fig. 1.5. The east-west distance between a peak and a valley is 180 km and the north-south is 360 km at least. The corresponding wavelengths will be 360 and 720 km respectively, which are somewhat larger than those estimated from the Aries observations. At the same time Katz's (1973) profiles suggest that small scales may have slightly (±10 km) contaminated Fuglister's (1960) sections. It is very interesting to notice that the strong gradient in tow 300 in Fig. 1.5 along 64° 50'W approximately is not found in the nearest section at 66°W, indicating that Katz's profiles as well as the wiggles in Fuglister's sections are not permanent.

During the U.S.S.R. POLYGON experiment in the tropocal North Atlantic a large-scale anti-cyclonic velocity disturbance was observed and Fig. 1.6 shows the average speed

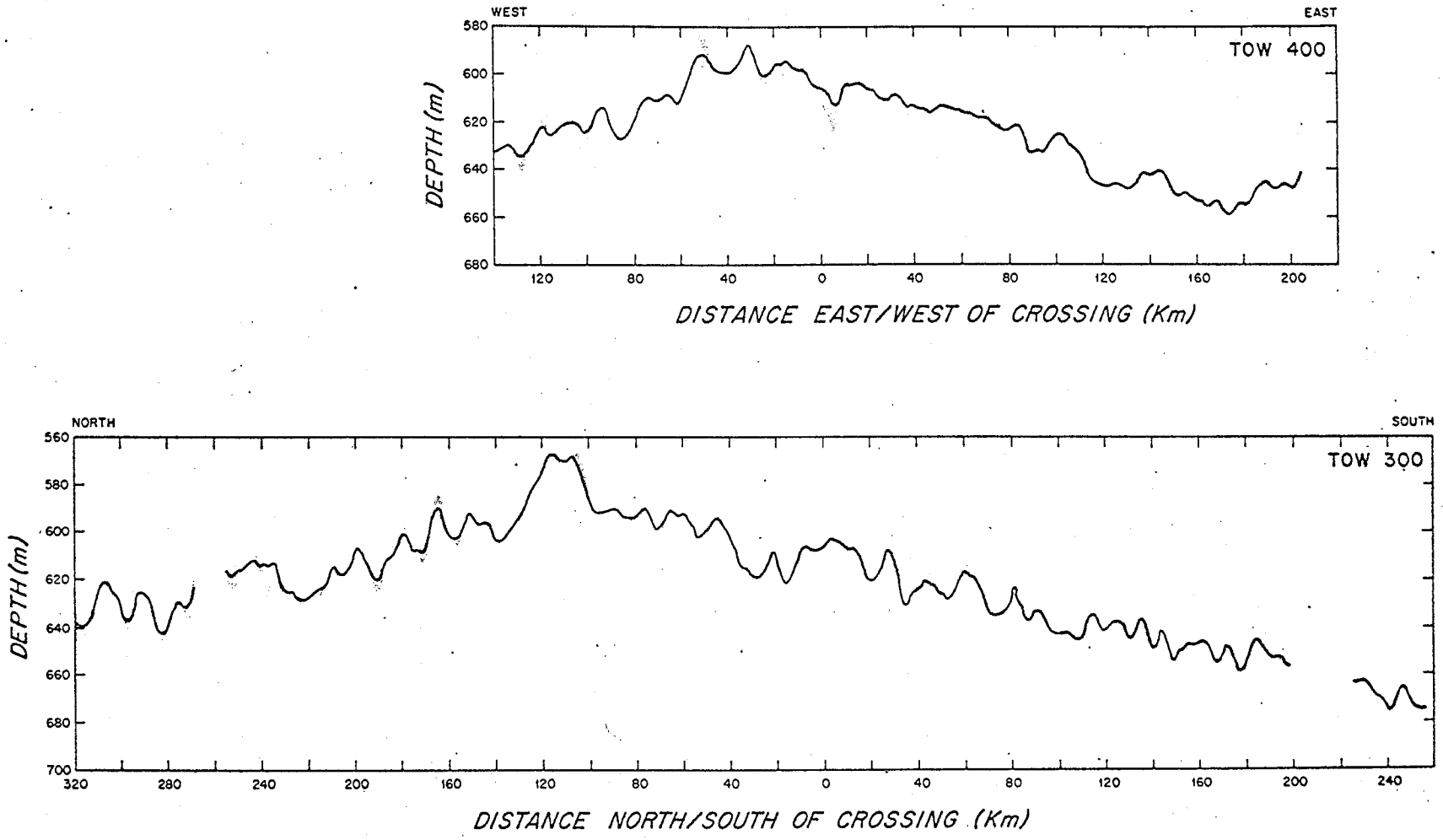

Fig. 1.5 From Katz(1973). Depth of isopycnals, σ_t= 26.91 for Tow 300 and σ_t=26.87 for Tow 400. These profiles confirm the presence of an intermediate scale. The distance between a peak and a valley is 180 km from Tow 400 and 360 km from Tow 300 at least.

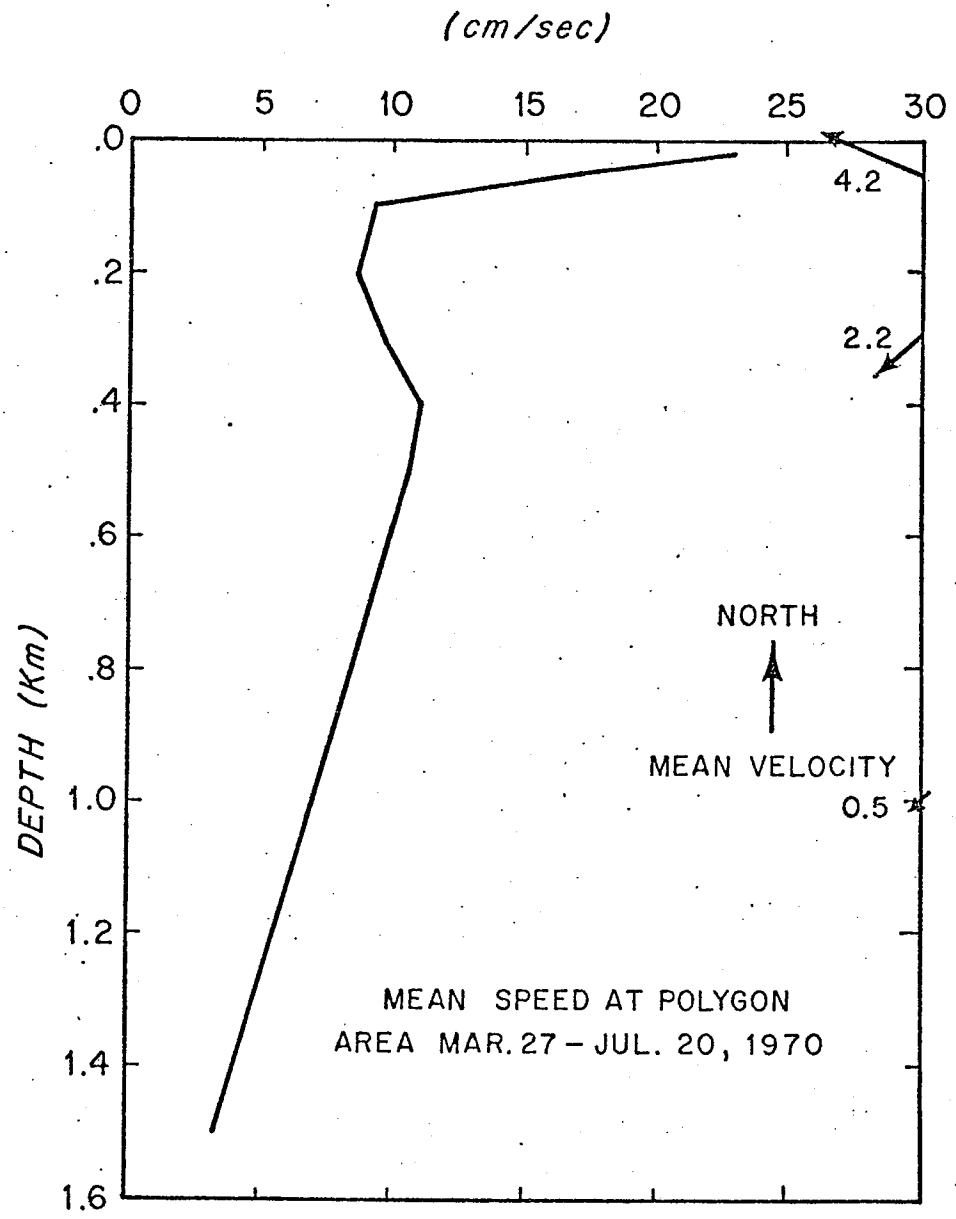

Fig. 1.6 Profile of mean speed and mean velocity plotted from Koshlyakov and Grachov(1973). A large-scale anti-cyclonic eddy was observed during the Polygon experiment and its mean speed is overwhelmingly larger than mean velocity for all depth. The main thermocline is located at about 250 m.

overwhelmingly larger than the average velocity from the surface to 1500 m depth. This is another important disclosure because the thermocline in the Polygon area is located at about 250 m, compared with about 800 m in the Sargasso Sea and the mean horizontal density gradient is much weaker by an order of magnitude.

Gould, Schmitz and Wunsch (1974) have suggested from estimates of vertical coherence of currents that the low frequency currents are usually dominated by the barotropic and first few baroclinic modes. The vertical profile of current in Fig. 1.7 from Sanford (1975) shows a very strong shear in the main thermocline which tends to justify the use of a simplified vertical structure in the present theory (two-layer ocean).

Bernstein and White (1974) reported oceanic subsurface perturbations in the central North Pacific and argued that these fluctuations are the manifestation of non-dispersive baroclinic planetary waves.

In summary, the last two decades' observations in the mid-ocean have consistently revealed the presence of energetic eddies with time scales of tens of days, length scales of tens to hundreds of kilometers and a strong vertical variation, irrespective of where and when the data were taken. The description of eddies is very subjective and indefinite because most experiments were in-